Supplementary Information

Supplementary Figures

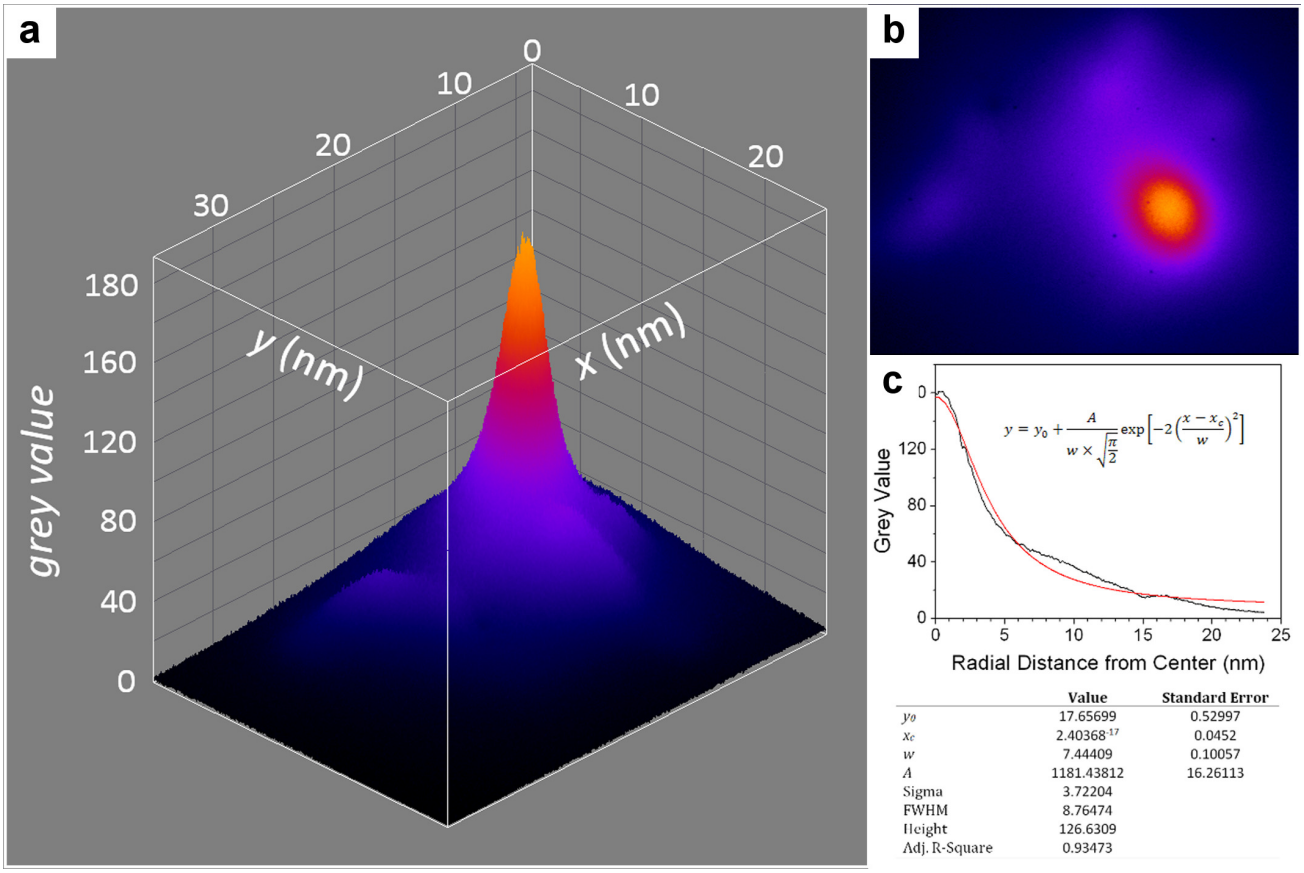

Supplementary figure S1: Characterisation of the electron beam intensity profile. (a) A 3D plot of beam intensity (grey value) with position, (b) the beam intensity recorded on the CCD detector; this image contains > 90% of the total beam intensity. (c) A cross section plot with a fitted Lorentzian curve used to determine a characteristic radius for the beam. The total beam current recorded on the Faraday cup was measured as 1 nA, corresponding to 6.241×10^9 e^- s^{-1}. From the Lorentz fit we can extract a full width half maximum (FWHM) value of 8.67 nm, corresponding to an area of 59.4 nm^2. The beam current density (BCD) is found by dividing the total beam current by the area (= 6.241×10^9 / 59.4 e^- $s^{-1}.nm^{-2}$), which is approximately 1×10^8 e^- s^{-1} nm^{-2}. This is an average value since the beam profile is Lorentzian.

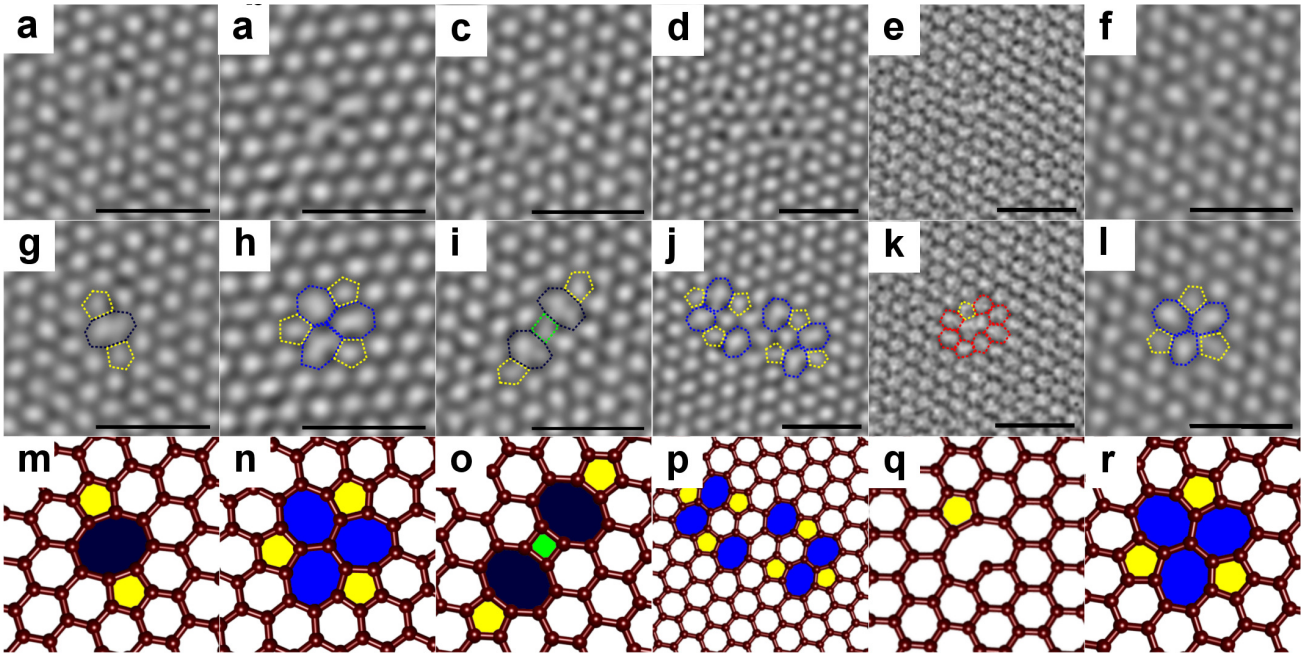

Supplementary figure S2: Defects created from 30 s exposure times. (a-f) Aberration-corrected transmission electron microscope (AC-TEM) images of defects formed after 30 s exposure to the focussed electron beam. (g-l) Annotated versions of (a-f). (m-r) Atomic models of the defects shown in (a-f). Defects shown in (a-c) are the same as those in figure 2 of the main text. The colour scheme denotes the number of carbons in the respective carbon ring, such that green, yellow, blue and dark blue represent 4-, 5-, 7- and 8-membered carbon rings, respectively. Scale bars denote 1 nm.

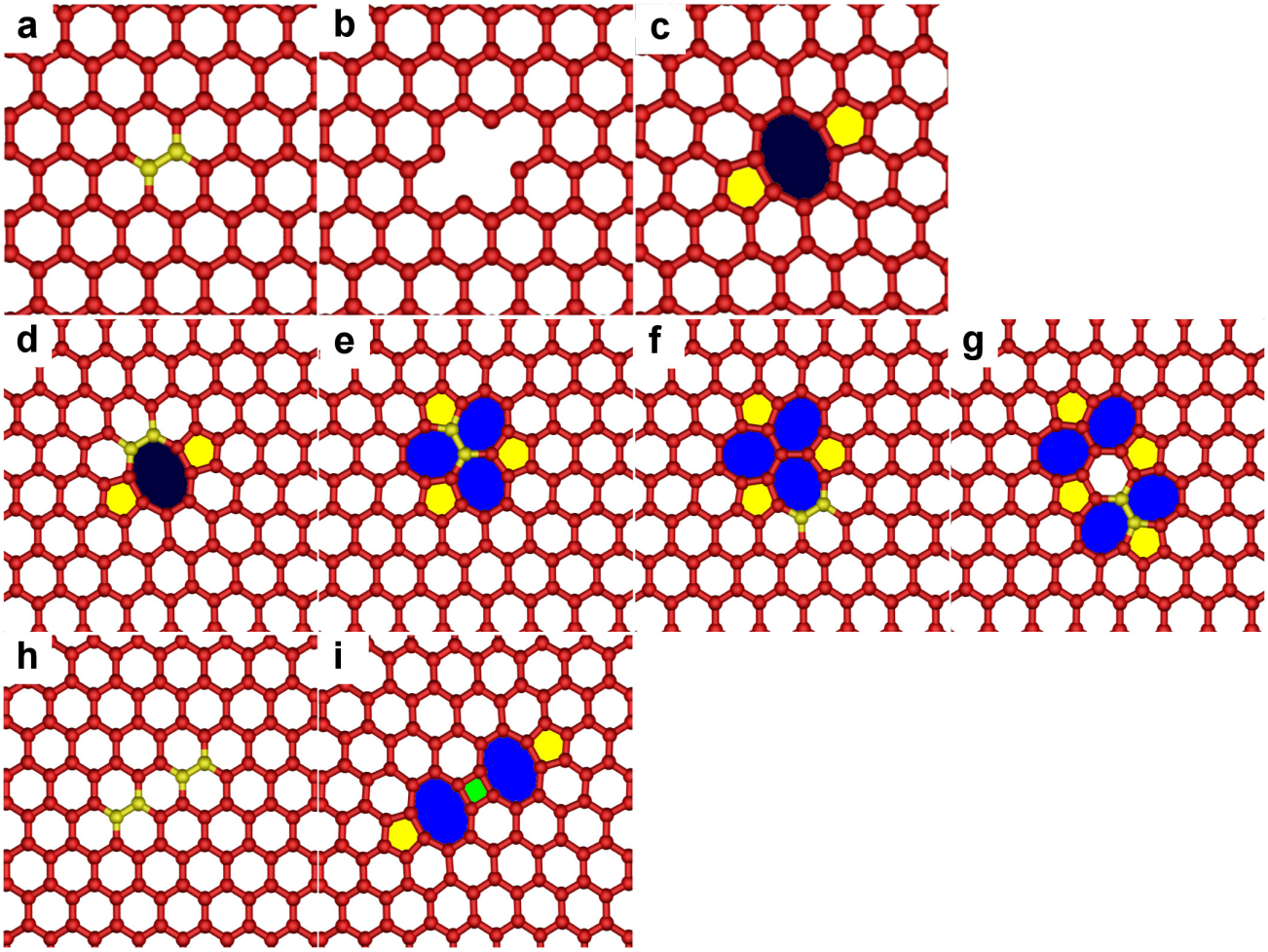

Supplementary figure S3: Atomistic models of defect formation. (a-c) Schematic models showing how a divacancy is formed (atoms displaced highlighted in gold), and (d-g) models showing a divacancy transforming via successive Stone-Wales rotations (bond rotated between frames indicated in gold). No further carbon atoms are lost in these transformations. (h,i) Schematic models showing how the removal of two carbon dimers (gold) along the arm-chair lattice direction of graphene leads to an extended, double divacancy armchair defect structure. The colour scheme denotes the number of carbons in the respective carbon ring, such that green, yellow, blue and dark blue represent 4-, 5-, 7- and 8-membered carbon rings, respectively.

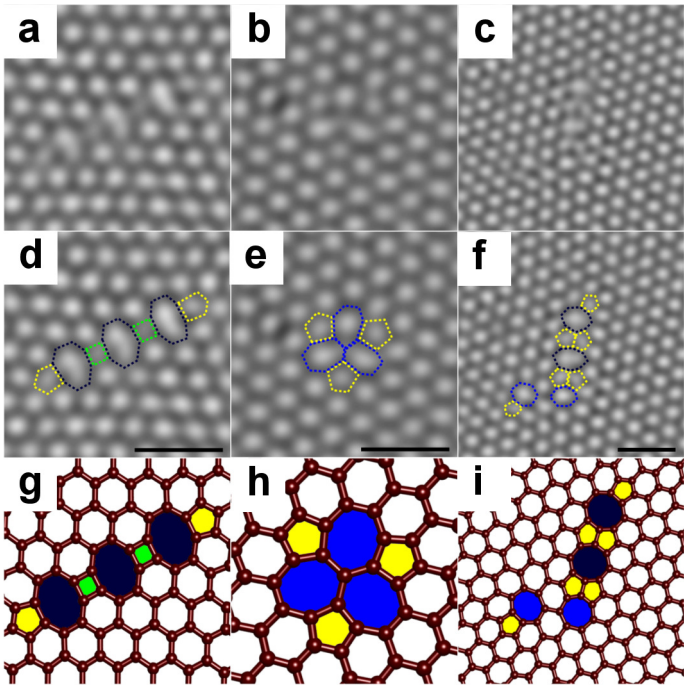

Supplementary figure S4: Defects created after 60 s exposure. Aberration-corrected transmission electron microscope (AC-TEM) images of defects formed after 60 s exposure to the focussed electron beam. Defects shown in (a-c) are the non-annotated versions of the images shown in figure 3 of the main text, also shown in (d-f). (g-i) Atomistic models of (a-c). The colour scheme denotes the number of carbons in the respective carbon ring, such that green, yellow, blue and dark blue represent 4-, 5-, 7- and 8-membered carbon rings, respectively. Scale bars denote 1 nm.

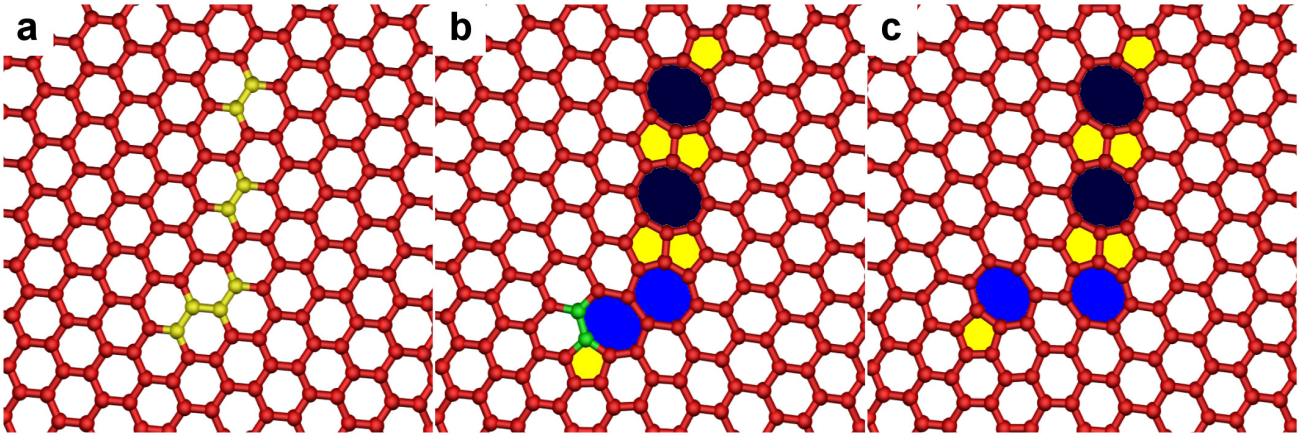

Supplementary figure S5: Atomistic models of defect creation. Schematic models demonstrating how the defect structure in figure 3c was formed. (a) Highlighted atoms that are sputtered, (b) the highlighted green bond rotated to form the observed defect, leading to the sliding of the dislocation, shown in (c). The colour scheme denotes the number of carbons in the respective carbon ring, such that yellow, blue and dark blue represent 5-, 7- and 8-membered carbon rings, respectively.

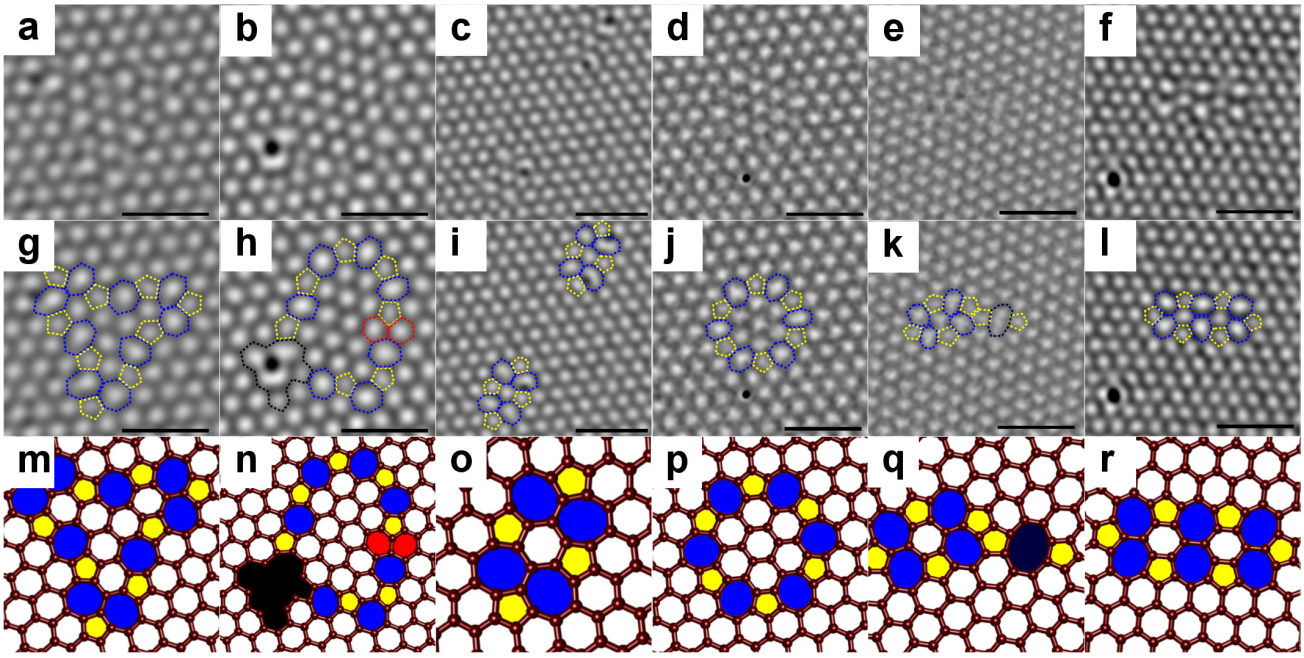

Supplementary figure S6: Defects created after 120 s exposure. (a-f) Aberration-corrected transmission electron microscope (AC-TEM) images of defects formed after 120 s exposure to the focussed electron beam. (g-l) Annotated versions of (a-f). (m-r) Atomic models of the defects shown in (a-f). Defects shown in (a-c) are the same as those in figure 3 of the main text. The colour scheme denotes the number of carbons in the respective carbon ring, such that yellow, blue and dark blue represent 5-, 7- and 8-membered carbon rings, respectively. The red in (h,n) denotes 6-membered rings completing the closed loop. Scale bars denote 1 nm.

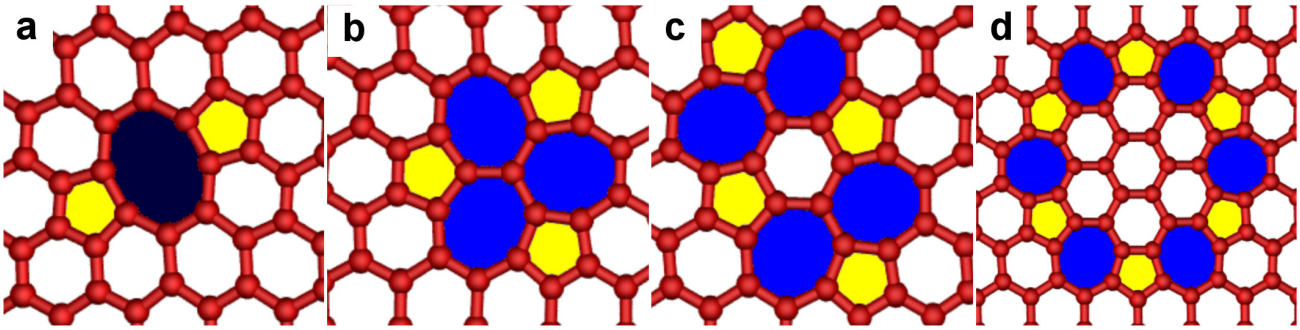

Supplementary figure S7: Normalised defect values for a selection of defects. (a-d) Schematic models of defect structures to illustrate normalised defect values. (a) 3; 3 non-6-membered rings. (b) 6; 6 non-6-membered rings. (c) 9; 8 non-6-membered rings + 1 rotated 6-membered ring. (d) 19; 12 non-6-membered rings + 7 rotated 6-membered rings. Due to divacancy defects shifting between (a), (b) and (c) on short time scales and under imaging beam current densities, a mean defect value of 6 was used for any single, isolated divacancy defect. The colour scheme denotes the number of carbons in the respective carbon ring, such that yellow, blue and dark blue represent 5-, 7- and 8-membered carbon rings, respectively.